

FINITE ELEMENT MODELLING FOR COLD FORM STEEL COLUMN WITH THE WEB AND FLANGE STIFFENER

Mohd Nasir Hussin, Algooda Ahmed Gamal & Mohd Emierul
Infrastructure University Kuala Lumpur, MALAYSIA

ABSTRACT

Cold-formed steel sections are a cost-effective alternative to traditional wood sections, which are mostly utilized in residential structures, and employed in industrial applications. Several unique items have been produced from it. While experimental testing is presently the most reliable approach for studying the behaviour of CFS sections, its effectiveness is limited by the expense of research. There aren't enough studies that use laboratory testing or numerical analysis to investigate the behaviour of CFS sections. As a result, it is more important than ever to utilize Finite Element Modelling (FEM) to simulate the realistic behaviour of CFS sections, especially when longer spans are necessary. While conducted under concentrically applied load and pin-ended boundary conditions, 36 axial compression tests were performed on CFS channels of three different lengths (1 m, 1.5 m, and 2 m) and four different cross-sections to investigate the interaction of local and overall flexural buckling in plain and lipped cold-formed steel (CFS) channels under axial compression. One sample was chosen from the real experiment to confirm the validity of FEM based on a physical experiment for the columns with lipped stiffener using FEM software based on real conducted experimental and nonlinear FE models about the CFS columns with lipped stiffener under the effect of axial load. The obtained FEM results for the ultimate capacity was 120.337 kN, and the percentage error for the FEM 5.8%. Furthermore, a parametric study was conducted for 3 samples of cold-formed steel with intermediate stiffener in the web and lipped in the flange with different angles for the intermediate stiffener and the ultimate capacity was recorded for the three samples was between 200-211kN. Moreover, that present load vs. displacement for samples A, B, and C combined which had an ultimate strength of (1.09621, 211.069), (1.08838, 206.481), and (1.07742, 199.975) respectively.

Keywords:

Cold Formed Steel, Finite Element Model, Parametric study

INTRODUCTION

Cold-Formed Steel (CFS) sections have become well-established in building construction due to its excellent structural performance, corrosion resistance, ease of manufacture, maintenance, and attractive appearance and lightweight. CFS trusses are commonly used as roof structures in industrial and residential buildings. Researchers discovered in the early 21st century that by combining the CFS with other materials, such as concrete, the structural performance of the CFS could be considerably enhanced (Amsyar et al., 2018). Commonly, CFS also known as Light Gauge Steel or LGS, is used for structural framing in structures of all sizes and purposes all over the world. Multi-story constructions, engineering conformity with local design and building standards, and the ability to survive if any structure constructed with traditional materials are among them. CFS sections are a cost-effective alternative to traditional wood sections, which are mostly utilized in residential structures, and employed in industrial applications. Several unique items have been produced, including C, Z, hat, and more specific chord and web parts, as shown in Figure 1. Furthermore, welding, adhesives, mechanical connectors such as bolts or screws, or even new mechanical connecting techniques such as press joining or rosette joining can all be used to make the connections (Hancock, 2016).

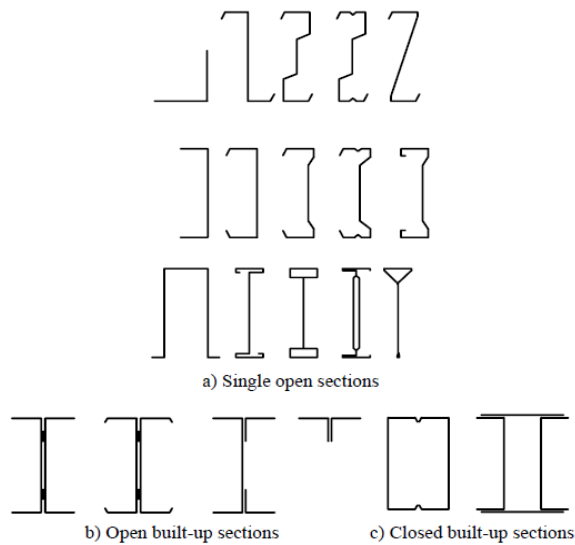


Figure 1: Typical Forms of Cold-Formed Sections

While experimental testing is presently the most reliable approach for studying the behaviour of CFS sections, its effectiveness is limited by the expense of research. There aren't enough studies that use laboratory testing or numerical analysis to investigate the behaviour of CFS sections. As a result, it is more important than ever to utilize Finite Element Modelling (FEM) to simulate the realistic behaviour of CFS sections, especially when longer spans are necessary. In this paper, FEM will be utilized to perform tests on CFS channels with stiffeners and show their behaviour under compressive load.

LITERATURE REVIEW

Material Properties

The study by Ma et al. (2015) discusses the material characteristics and residual stress distributions of cold-formed high-strength steel hollow sections. On high-strength steel hollow sections in rectangular, square, and circular shapes cold-forming effects have been investigated. Cold-formed structural hollow sections were evaluated using 66 standard tensile coupon tests, which evaluated the material characteristics of the high-strength steel structural hollow sections. Flat and corner coupons were machined out of the SHS and RHS, while curved coupons were machined out of the CHS, depending on the cross-sectional shape as illustrated in Figure 2. For the flat tensile coupon testing, the test pieces were 6 mm broad and 25 mm in gauge length. For the corner and curved tensile coupon tests, the corner and curved tensile coupons were 4 mm wide throughout the gauge length of 25mm.

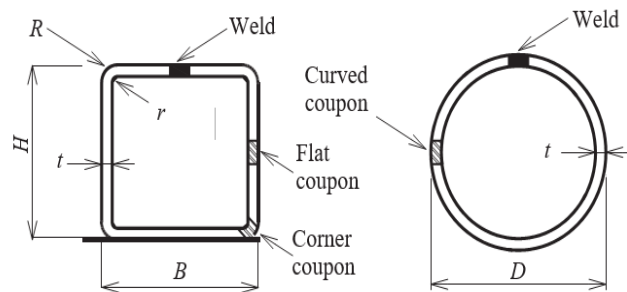


Figure 2: Tensile Coupons Locations

Buckling of CFS

Using an experimental study and finite element analysis on evenly lipped angles squeezed between fixed ends for different column lengths, (Young & Ellobody, 2005) investigated the buckling behaviour of CFS. The lipped angle test specimens were produced from brake-pressed zinc-coated structural steel sheets. The specimens were cut into lengths ranging from 250 to 3,500 mm. Three distinct lipped angles were investigated, each having a nominal flange width of 70 mm and a nominal lip width of 15 mm. The nominal plate thicknesses were 1.2, 1.5, and 1.9 mm. The nonlinear finite element model was validated using recent experimental data.

While (Ye, Hajirasouliha, et al., 2018) conducted under a concentrically applied load and pin-ended boundary conditions, 36 axial compression tests were performed on CFS channels of three different lengths (1 m, 1.5 m, and 2 m) and four different cross-sections. The investigation was on the interaction of local and overall flexural buckling in plain and lipped CFS channels under axial compression. The findings were utilized to confirm the validity of Eurocode 3 existing design methods. All the specimens that were examined were made with similar coil width and thickness.

All 36 specimens had local buckling, which was followed by failure owing to the interaction of local and overall flexural buckling around the minor axis. No distortional buckling was evident in any of the investigated cross-sections, even at late stages of post-peak behaviour. The local buckling deformations concentrated towards mid-height in the last phases of the testing, and a yield line mechanism formed. The failed geometries of the 1 m long specimens are shown in Figure 2.



Figure 2: The Failed Specimens with 1 Meter Long

Finite Element Model (FEM)

A numerical study and design of CFS built-up closed section columns with web stiffeners is presented in (Zhang & Young, 2018) research. To predict the structural behaviour of fixed-ended built-up closed section compression members, a finite element model (FEM) was created that considered initial geometric defects and nonlinear material characteristics. In this research, the ABAQUS finite element software was utilised to create a finite element model that was used to examine the structural behaviour of fixed-ended built-up closed section compression members. The FEA was carried out in two stages. First, a linear perturbation analysis was used to conduct an eigenvalue buckling analysis. The ultimate strength and failure mechanism of a built-up closed section column were predicted using a nonlinear approach. The generated FEM was validated against the test findings for cold-formed steel built-up closed sections by comparing the predictions of the FEA column strengths (PFEA) with the experimental results (PEXP). A total of 26 cold-formed steel built-up closed sections with inner and outward web stiffeners were used in this research, as shown in Figure 3.

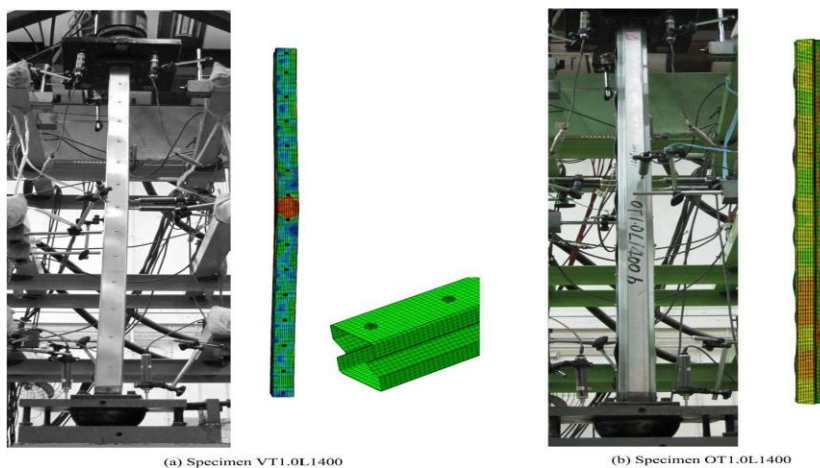


Figure 3: Experimental and Finite Element Analysis Deformation Forms of Built-Up Closed Section

The nonlinear behavior and design of built-up cold-formed steel section battened columns are discussed in (Dabaon et al., 2015) article. The pin-ended built-up columns were made from two cold-formed steel channels that were put back-to-back and connected by batten plates. The behavior of the built-up CFS section battened columns were modeled using the finite element software ABAQUS. Individually, the cold-formed steel channels, batten plates, and end loading plates were defined. The slender cold-formed steel channels (chords) and batten plates were modeled using the S4R shell element from the ABAQUS element collection. The models considered the nonlinear material characteristics of the flat and corner sections of the channels, as well as starting geometric imperfections, actual geometries, and boundary conditions. The finite element models were compared to tests on the same kind of section that the authors had previously performed and reported on, as shown in Figure 4.

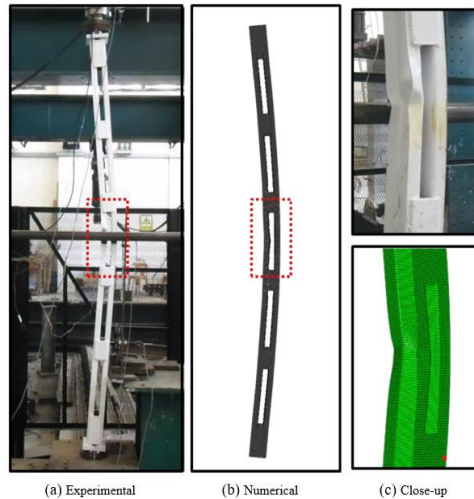


Figure 4: The Built-Up Column Deformed Shape

RESEARCH METHODOLOGY

Verification of the Finite Element Model

Based on the experimental testing results presented by (Ye, Hajirasouliha, et al., 2018) for buckling in CFS lipped channels under axial compression with pin-ended boundary conditions the ultimate capacity for specimen A1000-a is 99.8 kN as demonstrated in section 3.7. Moreover, a follow-up FEM study to the experimental testing results was conducted by researchers (Ye, Mojtabaei, et al., 2018), which followed the same conditions, the ultimate capacity was 113.7 kN. On the other hand, the FEM study conducted under this thesis went through the same conditions of the experimental study. Furthermore, the obtained FEM results for the ultimate capacity that was carried out in section 3.6 for specimen A1000-a produced an ultimate capacity of 120.337 kN. Therefore, the percentage error between the FEM results for the ultimate capacity is 5.8% as shown in Table 1.

Table 1: Differences in ultimate load capacity between Controlled sample and FEM

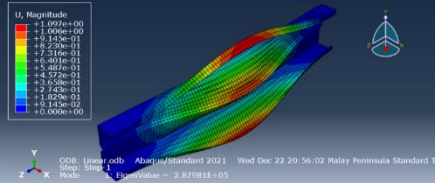
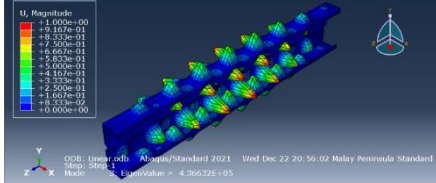
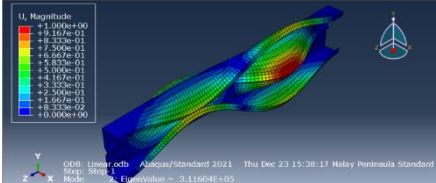
Specimen A1000-a	Ultimate load capacity	Percentage
Experimental sample conducted by (Ye, Hajirasouliha, et al., 2018)	99.8 kN	
FEM conducted by (Ye, Mojtabaei, et al., 2018)	113.7 kN	$\frac{113.7 - 99.8}{99.8} \times 100 = 14\%$

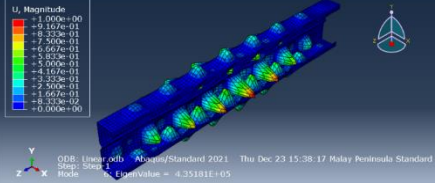
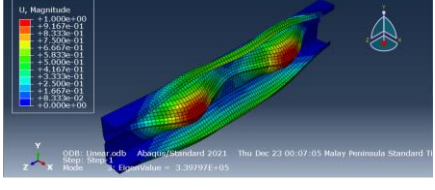
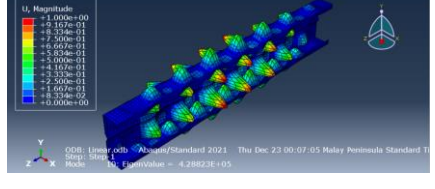
FEM study conducted in this study	120.337 kN	$\frac{120.3 - 99.8}{99.8} \times 100 = 20.58\%$ $\frac{120.3 - 113.7}{113.7} \times 100 = 5.8\%$
-----------------------------------	------------	---

Parametric Study

The parametric study of the three samples, a linear analysis was conducted with 10 eigenvalues to obtain the buckling type. Furthermore, the first eigenvalues for each sample used a nonlinear analysis to obtain the ultimate capacity and compare it between the three samples to investigate the most suitable intermediate stiffener angle in the web, as shown in Table 2.

Table 2: Result of the parametric study

Sample	Ultimate capacity	Mode	Type of buckling
<p>A</p> <p>Column with the web and flange stiffener.</p> <p>(Intermediate stiffener angle 45°)</p>	211.1 kN	1 st -2 nd	 <p>Global buckling</p>
		3 rd -10 th	 <p>Local buckling</p>
<p>B</p> <p>Column with the web and flange stiffener.</p>	206.5 kN	1 st -5 th	 <p>Global buckling</p>

(Intermediate stiffener angle 37°)		6 th -10 th	 <p style="text-align: center;">Local buckling</p>
C Column with the web and flange stiffener.	200 kN	1 st -8 th	 <p style="text-align: center;">Global buckling</p>
		9 th -10 th	 <p style="text-align: center;">Local buckling</p>

Vertical Displacement

The typical load-displacement curve for each sample obtained from the tests and the ultimate loads among the three samples and various displacements are shown in Figure 5.

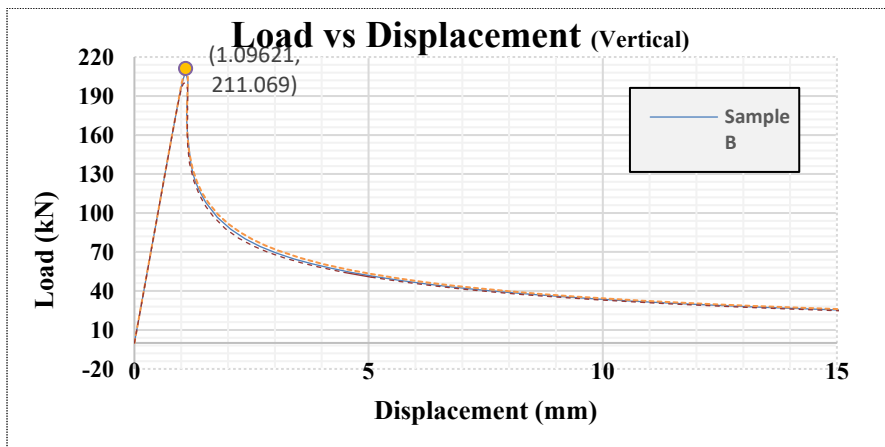


Figure 5: Load vs Displacement for sample A, B and C

DISCUSSION

Verification of the Finite Element Model

Based on the experimental testing results presented by Ye Hajirasouliha et al. (2018), when conducting a study that focuses on the interaction of local and overall flexural buckling in CFS lipped channels under axial compression that concentrically have an applied load and pin-ended boundary conditions, the corresponding obtained results for the ultimate capacity for specimen A1000-a is 99.8 kN as demonstrated in Figure 6. Moreover, a follow-up FEM study to the experimental testing results was conducted by Ye Hajirasouliha et al. (2018), which followed the same conditions of the experimental study to provide a more comprehensive overview on the buckling in CFS lipped channels. Therefore, the obtained FEM results for the ultimate capacity for specimen A1000-a was 113.7 kN, as illustrated in Figure 6. Therefore, the FE simulated load capacity ratio to the experimentally measured load-carrying capacity was 1.139, and the percentage error is 13.9% \approx 14%. On the other hand, in the FEM study conducted in this investigation which followed the same conditions of the experimental study, the obtained FEM results for the ultimate capacity that was carried out for specimen A1000-a produced an ultimate capacity of 120.337 kN. Hence, the FEM simulated load capacity ratio in this study to the experimentally measured load-carrying capacity was a 20% percentage difference. Furthermore, the percentage difference between the FEM results from Ye Hajirasouliha et al. (2018) and this study for the ultimate capacity is 5.8%. However, by using a much higher mesh number while performing the simulation analysis can further reduce the percentage difference.

Specimen	Length (mm)	P_u (test) (kN)	P_{u1} (FE) (kN)
A1000-a	1000.1	99.8	113.7
A1000-b	1000.0	98.3	117.5
A1000-c	1000.0	98.7	114.9
A1500-a	1499.8	95.1	89.8
A1500-b	1500.0	85.3	81.9
A1500-c	1500.0	91.4	94.06
A2000-a	1999.8	78.4	88.4

Figure 6: Results Obtained by (Ye, Mojtabaci, et al., 2018)

Parametric Study

Table 2 summarised the obtained FEM results for the designed samples. All samples showed improvement in the ultimate capacity after adding the intermediate stiffener in the web which was recorded between 200-211kN for all samples. Sample A with 45° of the intermediate stiffener recorded the highest ultimate capacity of 211kN followed by sample B with 37° that recorded an ultimate load of 206.5kN. Sample C with 30° on the other hand presented the lowest ultimate capacity of 200kN. Hence, the comparison clearly indicates that the 45° intermediate stiffeners present the best ultimate capacity. The observed failure mode presented in Table 2 showed local buckling and global buckling for all three samples.

Vertical Displacement

Researchers (e.g., Aulia & Rinaldi, 2015) presented that a structure's ductility can be considered one of the most essential factors determining its performance and capabilities. Ductility refers to a structure's capacity to produce post-yield deformation before buckling, and it may become the most crucial element in determining damage level. However, as can be seen from Figure 5, that present load vs. displacement for samples A, B, and C combined which had an ultimate strength of (1.09621, 211.069), (1.08838, 206.481), and (1.07742, 199.975) respectively. The behaviour of the designed CFS column with the different intermediate stiffener angles for the load-displacement graph had approximately the same displacement characteristics due to the insignificant intermediate stiffener angles for samples A, B, and C.

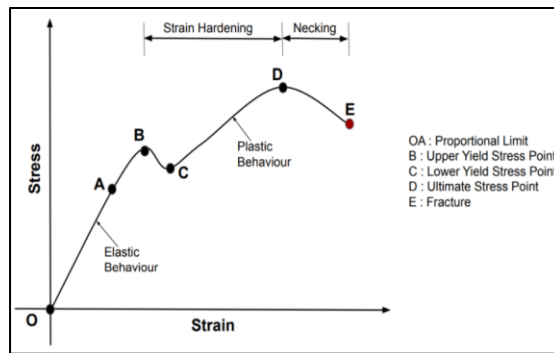


Figure 7: Stress vs Strain Curve

As it can be seen from Figure 7, which demonstrates the Stress-Strain curve for ductile materials, the proportional limit (O-A), according to Hooke's Law, is the point at which stress is directly proportional to strain which makes the stress-strain curve in a straight line within the proportional limit at this region. From point A to B (Yield Point) on the stress-strain curve, the material has elastic characteristics. After the external force is removed, the material will not return to its previous form. If the external load (stress) is increased above the elastic limit. Plastic qualities appear when ductile material is stretched beyond its elastic limit. The higher yield point is the point at which the material's maximum tension is needed to cause plastic deformation. Yield strength is the strength of a material that corresponds to Point B.

Moreover, Plastic properties appear when ductile material is stretched beyond its elastic limit. The higher yield point is the point at which the material's maximum tension is needed to cause plastic deformation. Yield strength is the strength of a material that corresponds to Point B. With a minor increase in tensile force after Point C, the material length will rise (stress). In other words, the Lower Yield Point is the point at which the minimal load is necessary for the material to display plastic behaviour. The ultimate tensile strength of the material is shown by the material strength corresponding to Point D on the stress-strain diagram. A material's ultimate tensile strength is the utmost stress it can bear before breaking. Inside the material, necking begins after point D.

Therefore, since there were no major differences between sample A, B, and C, in load-displacement and stress-strain curves, sample A can be taken as an example to explain the obtained results characteristics across different regions. The point A proportional limit in the Figure 4.6, stress-strain graph for sample A is (0, 195.675) and before this point is the elastic behaviour for the CFS column. The point B, upper yield stress point is (0.00011, 201.01), and before this point is the elastic limit. For the point C, lower yield stress point is (0.00195, 95.902). The ultimate stress in the sample A is (0.0142, 273.673) which represent the point D in the graph.

CONCLUSION

To conclude, the study's objectives were accomplished successfully by simulating a column with the lipped in the flange. The study was on the behaviour of CFS with the lipped stiffener in terms of buckling. The experimental testing results of the buckling in CFS lipped channels under axial compression with pin-ended boundary conditions had an ultimate capacity for specimen A1000-a is estimated by 99.8 KN, followed up by FEM study to the experimental testing results by researchers Ye Hajirasouliha et al. (2018), which followed the same conditions. The ultimate capacity in this case, was 113.7 KN. However, the obtained FEM results for the ultimate capacity carried out under this research in for specimen A1000-a produced an ultimate capacity of 120.337 kN. Therefore, the percentage difference between the FEM results for the ultimate capacity is 5.8%. Which summarizes the first objectives of the study, to produce a nonlinear FEM analysis based on a physical experiment and verifying the validity/ workability of the software simulation.

Furthermore, the second objective was met by making 3 samples of CFS columns with intermediate stiffeners in the web and lipped in the flange by using Abaqus software to show the buckling behaviour under axial load which all were included under the parametric study. The samples maintained the same nominal thickness ($t=1.5\text{mm}$), coil width and height ($L=1000\text{mm}$) as the original specimen A1000-a was included in the study but with additional intermediate stiffeners in the web. Additionally, the 3 samples had different angles of the intermediate stiffeners to validate the study with the best angle consideration. However, the geometric limitation of the sample was based on the study conducted by (Wang & Young, 2014) for the CFS channel sections with web stiffeners.

All samples showed improvement in the ultimate capacity after adding the intermediate stiffener in the web which was recorded between 200-211kN for all samples. Sample A with 45° of the intermediate stiffener recorded the highest ultimate capacity of 211kN followed by sample B with 37° that recorded an ultimate load of 206.5kN. Sample C with 30° on the other hand presented the lowest ultimate capacity of 200kN. Hence, the comparison clearly indicates that the 45° intermediate stiffeners present the best ultimate capacity.

The third objective was accomplished by examining the vertical displacement of the three samples, which revealed that the load-displacement graph behaviour of the proposed CFS column with various intermediate stiffener angles had almost comparable displacement characteristics. Furthermore, for each sample corresponding to the width of the angle, the stress vs strain analysis revealed various upper/lower yield stresses, ultimate stresses, and fracture points.

AUTHOR BIOGRAPHY

Mohd Nasir Hussin, Assoc. Prof, Ir., is Associate Professor in Infrastructure University Kuala Lumpur. His expertise is in reinforced design and infrastructure.

Algooda Ahmed Gamal is a final year student at Infrastructure University Kuala Lumpur. He is studying in Bachelor of Civil Engineering (Hons).

Mohd Emierul, Ts., is a lecturer in the Civil Engineering & Construction Department of Infrastructure University Kuala Lumpur. His expertise is in reinforced design and infrastructure.

REFERENCES

- Amsyar, F., Tan, C. S., Ma, C. K., & Sulaiman, A. (2018). Review on Composite Joints for Cold-Formed Steel Structures. *E3S Web of Conferences*, 65, 08006.
- Billah, M., Islam, M. M., & Ali, R. B. (2019). Cold formed steel structure: An overview. *World Scientific News*, 118, 59–73.
- Dabaon, M., Ellobody, E., & Ramzy, K. (2015). Nonlinear behaviour of built-up cold-formed steel section battened columns. *Journal of Constructional Steel Research*, 110, 16–28.
- Dawe, J. L., Liu, Y., & Li, J. (2010). Strength and behaviour of cold-formed steel offset trusses. *Journal of Constructional Steel Research - J CONSTR STEEL RES*, 66, 556–565.
- Fratamico, D. C., Torabian, S., Zhao, X., Rasmussen, K. J. R., & Schafer, B. W. (2018). Experiments on the global buckling and collapse of built-up cold-formed steel columns. *Journal of Constructional Steel Research*, 144, 65–80.
- Hancock, G. (2016). Cold-formed steel structures: Research review 2013–2014. *Advances in Structural Engineering*, 19(3), 393–408.
- Kang, T. H.-K., Biggs, K. A., & Ramseyer, C. (2013). Buckling Modes of Cold-Formed Steel Columns. *International Journal of Engineering and Technology*, 477–451.
- Konkong, N., Aramraks, T., & Phuvoravan, K. (2017). Buckling length analysis for compression chord in cold-formed steel cantilever truss. *International Journal of Steel Structures*, 17(2), 775–787.
- Ma, J.-L., Chan, T.-M., & Young, B. (2015). Material properties and residual stresses of cold-formed high strength steel hollow sections. *Journal of Constructional Steel Research*, 109, 152–165.
- Moen, C. D., & Schafer, B. W. (2008). Experiments on cold-formed steel columns with holes. *Thin-Walled Structures*, 46(10), 1164–1182.
- Ye, J., Hajirasouliha, I., & Becque, J. (2018). Experimental investigation of local-flexural interactive buckling of cold-formed steel channel columns. *Thin-Walled Structures*, 125, 245–258.
- Ye, J., Mojtabaei, S. M., & Hajirasouliha, I. (2018). Local-flexural interactive buckling of standard and optimised cold-formed steel columns. *Journal of Constructional Steel Research*, 144, 106–118.
- Young, B., & Ellobody, E. (2005). Buckling Analysis of Cold-Formed Steel Lipped Angle Columns. *Journal of Structural Engineering*, 131(10), 1570–1579.
- Zhang, J.-H., & Young, B. (2018). Finite element analysis and design of cold-formed steel built-up closed section columns with web stiffeners. *Thin-Walled Structures*, 131, 223–237.
- ABAQUS Theory Manual, v6.6. http://130.149.89.49:2080/v6.11/pdf_books/THEORY.pdf. (2011).
- Aulia, T. B. & Rinaldi. (2015). Bending Capacity Analysis of High-strength Reinforced Concrete Beams Using Environmentally Friendly Synthetic Fiber Composites. *Procedia Engineering*, 125, 1121–1128. <https://doi.org/10.1016/j.proeng.2015.11.136>
- Wang, L., & Young, B. (2014). Cold-formed steel channel sections with web stiffeners subjected to local and distortional buckling - Part II: Parametric study and design rule. *22nd International Specialty Conference on Recent Research and Developments in Cold-Formed Steel Design and Construction*, 243–257